Journal of Experimental Botany, Vol. 60, No. 11, pp. 3031–3042, 2009
doi:10.1093/jxb/erp131 Advance Access publication 6 May, 2009
This paper is available online free of all access charges (see http://jxb.oxfordjournals.org/open_access.html for further details)

Journal of Experimental Botany
www.jxb.oxfordjournals.org

RESEARCH PAPER

Transient winter leaf reddening in *Cistus creticus* characterizes weak (stress-sensitive) individuals, yet anthocyanins cannot alleviate the adverse effects on photosynthesis

Konstantina Zeliou, Yiannis Manetas and Yiola Petropoulou*

Laboratory of Plant Physiology, Section of Plant Biology, Department of Biology, University of Patras, GR-265 00, Greece

Received 15 December 2008; Revised 27 March 2009; Accepted 5 April 2009

Abstract

Under apparently similar field conditions individual plants of *Cistus creticus* turn transiently red during winter, while neighbouring plants remain green. These two phenotypes provide a suitable system for comparing basic photosynthetic parameters and assessing critically two hypotheses, i.e. anthocyanins afford photoprotection and anthocyanins induce shade characteristics on otherwise exposed leaves. With that aim, pigment levels and *in vivo* chlorophyll fluorescence parameters were monitored in dark-acclimated (JIP-test) and light-acclimated (saturation pulse method) leaves during both the green and the red period of the year. No evidence for actual photoprotection by anthocyanins was obtained. On the contrary, all fluorescence parameters related to yields and probabilities of photochemical energy conversion and electron flow, from initial light trapping to final reduction of ultimate electron acceptors in PSI, declined in the red phenotype after leaf reddening. Moreover, the pool sizes of final electron acceptors of PSII diminished, indicating that both photosystems were negatively affected. Vulnerability to winter stress was also indicated by sustained chlorophyll loss, inability to increase the levels of photoprotective xanthophylls and increased quantum yield of non-regulated energy loss during reddening. However, during the same period, the relative PSII antenna size increased, indicating an apparent shade acclimation after anthocyanin accumulation, while changes in the photosynthetic pigment ratios were also compatible to the shade acclimation hypothesis. All parameters recovered to pre-reddening values upon re-greening. It is concluded that the photosynthetic machinery of the red leaf phenotype has an inherently low capacity for winter stress tolerance, which is not alleviated by anthocyanin accumulation.

Key words: *Cistus creticus*, electron transport, epoxidation state, OJIP curves, photoinhibition, photoprotection, pigments, PSI, PSII, shade acclimation.

Introduction

In some plants and under some circumstances, leaves may appear red due to accumulation of anthocyanins. These pigments absorb visible radiation without being photosynthetic, hence they compete with chlorophylls for photon capture and, accordingly, their presence entails a photosynthetic cost, equal to the lost photons. Yet, the cost of any conserved trait should be paid-off by a corresponding benefit. The adaptive significance of leaf redness, however, is not well understood. Ecologically oriented hypotheses link red leaf colour with the avoidance of overconsumption by folivorous insects (Archetti, 2000; Hamilton and Brown, 2001; Ougham *et al.*, 2005) and earned support from observations that young or senescing red leaves seem to be less attractive for food or oviposition (Archetti and Leather, 2005; Karageorgou and Manetas, 2006). Physiologically oriented hypotheses consider that anthocyanins are photoprotective, either as passive light screens or through their antioxidant function (Lee and Gould, 2002; Steyn *et al.*,

* To whom correspondence should be addressed: E-mail: petropo@upatras.gr

2002; Ougham *et al.*, 2008). They may act as a last line of defence against photoinhibitory damage when the first lines of defence (i.e. chloroplast and leaf movements, xanthophyll and water-water cycles, photorespiration) are not adequate or collapse. The photoprotective function is reasonable since in many cases the abundance of red leaves or red individuals is higher in exposed than in shaded sites (Kytridis *et al.*, 2008). Moreover, a variety of stresses that increase the photoinhibitory risk (nutrient deficiency, water or salt stress, high light in combination with cold temperatures) do induce the accumulation of anthocyanins in some plants (Manetas, 2006).

The photoprotective hypothesis was checked by examining whether red leaves are more tolerant of an applied photoinhibitory treatment in the laboratory. In most cases, a positive correlation between leaf redness and tolerance of photoinhibition has been reported (Krol *et al.*, 1995; Feild *et al.*, 2001; Manetas *et al.*, 2002; Pietrini *et al.*, 2002; Hughes *et al.*, 2005; Hughes and Smith, 2007), but see Burger and Edwards (1996) for a different result. However, the ultimate test for the sunscreen hypothesis is whether anthocyanin accumulation offers any actual photoprotection in the field. Results, again, are contradictory. Thus, Liakopoulos *et al.* (2006) reported a slight photoprotective function in young, developing *Vitis vinifera* leaves. Yet no evidence for an actual photoprotection was found in young leaves of *Quercus coccifera* (Manetas *et al.*, 2003), in mature leaves of *Prunus cerasifera* (Kyparissis *et al.*, 2007) and *Erythronium dens-canis* (Esteban *et al.*, 2008), and in senescing leaves of many woody species (Lee *et al.*, 2003). A by-product of these investigations (Gould *et al.*, 2002; Manetas *et al.*, 2003; Hughes and Smith, 2007; Kyparissis *et al.*, 2007) was that, irrespective of the likely function of the red-leaf trait, the anthocyanic screen imposes some morphological and physiological adjustments, partly compatible with the shade acclimation syndrome.

A slightly different version of the photoprotective hypothesis was recently adopted by Kytridis *et al.* (2008). These authors took advantage of the intra-species variation in the anthocyanic character displayed by the Mediterranean shrub *Cistus creticu*s, where mature leaves in some individuals turn transiently red during winter, while neighbouring individuals in the same site remain green. In this system, red individuals displayed slightly inferior photosynthetic and photoprotective capabilities and lower levels of leaf nitrogen. Yet, no sign of differential photoinhibitory damage between the two phenotypes was found. Thus, anthocyanin accumulation was assumed to compensate for the photosynthetic and photoprotective inferiority of the red plants through a light screen and/or an antioxidant function (Kytridis *et al.*, 2008).

In the present investigation, the photoprotective hypothesis and the assumed shade acclimation of red leaves were re-examined with the *C. creticus* system by using a new approach. Previous investigations used only the maximum PSII yield as a measure of photoinhibition, considering just two points in the fluorescence rise kinetics, i.e. the initial (F_0) fluorescence when all PSII centres are open and the maximum (F_M) fluorescence when all PSII centres close after a saturating light pulse. However, the fluorescence rise kinetics from F_0 to F_M is polyphasic, with characteristic steps denoting the step-wise flow of energy through PSII (Strasser *et al.*, 1995, 2004; Papageorgiou *et al.*, 2007) and up to the final electron acceptors of PSI (Jiang *et al.*, 2008; Tsimilli-Michael and Strasser, 2008; Yordanov *et al.*, 2008). If they are analysed appropriately by the so-called JIP-test, the original fluorescence data reveal several structural and functional attributes of PSII and PSI, which also encompass their donor and acceptor sides. Thus, additional information linked to photoinhibition and light/shade adjustments was sought by analysing the shape of the fast chlorophyll fluorescence transients.

It was also questioned whether the imposed anthocyanic screen would adjust the xanthophyll cycle pool sizes and the extent of diurnal inter-conversions of its components. Such adjustments accompany shade acclimation (Thayer and Björkman, 1990), and the corresponding information for red leaves is lacking. All parameters were monitored in both phenotypes at frequent intervals, starting just before the onset of reddening in early winter and ending at re-greening in late spring.

Materials and methods

Plant material study site and sampling protocol

Cistus creticus L. (Cistaceae) is an evergreen Mediterranean shrub pioneer on post-fire sites. The study area (38.14°N, 21.44°E, 250 m a.s.l.) was burnt in 1989 and today is covered by a mixture of short shrubs dominated by *C. creticus* and regenerating evergreen sclerophylls and pine trees. Previous observations (Kytridis and Manetas, 2006; Kytridis *et al.*, 2008) indicated that certain individuals of *C. creticus* turn red roughly at mid-winter and revert back to green at mid-spring. Hence, during this period, a field of *C. creticus* is a mosaic of green and red phenotypes. The frequency of red individuals is higher in the most well-lit sites and the anthocyanic trait is stable, i.e. the same shrubs turn red every year. This permits the permanent tagging of red and green plants to be studied both during the 'green' and the 'red' period of the year. Ten (five red and five green), south-facing shrubs were used throughout this study. Measurements started in early December 2007, i.e. 2 weeks before commencement of colour change, and ended in late summer 2008. As it is shown in Table 1, the mean monthly temperatures during the experimental period were comparable to the corresponding mean values over a period of 10 years in the study area.

Sampling was performed with a frequency of ~10 d during the first month and ⩾20 d afterwards, always on clear days. On each sampling date the site was visited twice, at mid-day and at pre-dawn of the following day; leaves were removed for pigment analysis and chlorophyll fluorescence measurements. Mature, exposed leaves were used throughout.

Table 1. Mean monthly temperatures (°C) for the study area during the experimental season and during the previous 10 years (1997–2006)

Temperature data were provided by the Regional Institute of Plant Protection (Patras).

	Nov	Dec	Jan	Feb	Mar	Apr	May	Jun	Jul	Aug
1997–2006	14.7	11.1	9.5	9.9	12.0	14.9	20.3	25.1	27.3	27.8
2007–2008	14.5	10.2	10.5	10.7	14.1	16.5	21.0	26.7	28.2	29.3

Pigment determination

Two leaves from every shrub (i.e. a total of 20 leaves, equally divided between red and green phenotypes), were harvested at midday and sampling was similarly repeated at pre-dawn of the following day. Both were immediately immersed in liquid nitrogen until extraction. They were extracted by grinding in a mortar with pure methanol plus a small amount of $CaCO_3$ under dim (0.3 μmol m^{-2} s^{-1}) light. After centrifugation at 5000 *g* for 10 min, the supernatant was further cleared by passing through 0.45 μm filters. Chlorophylls were measured spectrophotometrically in a Shimadzu (UV-160A) double-beam spectrophotometer by using the equations of Lichtenthaler and Wellburn (1983). A portion of the initial extract was acidified with concentrated HCl for spectrophotometric determination of anthocyanins according to Lindoo and Caldwell (1978). Carotenoid separation was performed with a Shimadzu LC-10 AD HPL chromatograph equipped with a calibrated, non-end-capped Zorbax ODS column and a photodiode array detector (Shimadzu, SPD-M10A_{VP}) as previously described (Manetas *et al.*, 2003).

Chlorophyll a fluorescence measurements

Six leaves from each tagged shrub (i.e. a total of 60 leaves, equally divided between red and green phenotypes) were sampled at pre-dawn of each sampling date and kept moistened in the dark for at least 1 h before measurement. Fast chlorophyll *a* fluorescence transients were induced by an array of six red (peak at 650 nm) LEDs, providing 3000 μmol photons m^{-2} s^{-1} for 2 s at leaf level. Fluorescence was captured by a Hansatech (Handy-PEA; Hansatech Instruments Ltd, King's Lynn, Norfolk, UK) analyser, recording with a time scan from 10 μs to 2 s and with a data acquisition rate of 10^5, 10^4, 10^3, 10^2, and 10 readings s^{-1} in the time intervals of 10–300 μs, 0.3–3 ms, 3–30 ms, 30–300 ms, and 0.3–2 s, respectively. The cardinal points in the fluorescence versus time curve used for further calculation of biophysical parameters were: maximal fluorescence intensity (F_M); fluorescence intensity at 20 μs, considered as the first credible measurement (F_0); fluorescence intensity at 300 μs ($F_{300\mu s}$) needed for calculation of the initial slope (M_0) of the relative variable fluorescence versus time curve; fluorescence intensity at 2 ms (i.e. at the J-step, F_J); fluorescence intensity at 30 ms (i.e. at the I-step, F_I). These primary data were used to derive the following parameters, according to the JIP-test (Strasser *et al.*, 2004; Jiang *et al.*, 2008; Tsimilli-Michael and Strasser, 2008; Yordanov *et al.*, 2008):

(i) The photosynthetic efficiencies at the onset of illumination, i.e. the maximum quantum yield of primary photochemistry $\varphi_{Po}=TR_0/ABS$, also known as F_V/F_M (where TR and ABS denote the trapped and absorbed excitation energy); the efficiency to conserve trapped excitation energy as redox energy (i.e. electron transfer, ET) $\psi_{Eo}=ET_0/TR_0$; the quantum yield of electron transfer to intermediate electron carriers $\varphi_{Eo}=ET_0/ABS = \varphi_{Po}\cdot\psi_{Eo}$; the efficiency of electron transfer between intermediate carriers to final acceptors of PSI, $\delta_{Ro}=R_{Eo}/ET_0$; and the quantum yield of reduction of final electron acceptors of PSI, $\varphi_{Ro}=\varphi_{Po}\cdot\psi_{Eo}\cdot\delta_{Ro}$.

(ii) The specific fluxes per active (i.e. Q_A-reducing) reaction centre (RC) for absorption (ABS/RC), trapping (TR_0/RC), electron transport (ET_0/RC), and dissipation (DI_0/RC).

The formulas used to calculate the above parameters are given in the Appendix.

Chlorophyll fluorescence measurements in the light acclimated state

During the middle of the 'red' period, leaves were sampled at pre-dawn, put in air-tight plastic bags and kept for at least 1 h in the dark. All further manipulations were done under dim background laboratory light of <1 μmol m^{-2} s^{-1}. Leaf discs were cut from both green and red leaves and placed in Petri dishes on moistened filter paper. An IMAGING-PAM (Walz, Effeltrich, Germany), equipped with blue LEDs providing measuring, actinic, and saturation pulse light, and a CCD camera for capturing the fluorescence was used. Before each measurement, the instrument probes the sample reflectance in the red and infrared band. A built-in equation is then used for the calculation of absorptance (*A*), to be used later in the calculation of linear electron transport rates. Following a saturation pulse for the measurement of dark-acclimated maximum PSII yield (as $F_V/F_M=(F_M-F_0)/F_M$), the sample was illuminated with step-wise increasing actinic irradiances, during which saturation pulses (0.8 s, 2400 μmol m^{-2} s^{-1}) were given every 60 s to close all PSII reaction centres. Duration of each actinic irradiance step was long enough for full photosynthetic induction, typically not <5 min. Light-acclimated PSII yield, Φ_{PSII}, was computed as $\Delta F/F_M'=(F_M'-F)/F_M'$ and linear electron transport rates as $ETR=\Phi_{PSII}\cdot PAR\cdot A\cdot 0.5$, where PAR is the incident photosynthetically active radiation, *A* the computed sample absorptance, and 0.5 a correction factor assuming equal light absorption by the two photosystems (Genty *et al.*, 1989). Both abaxial and adaxial leaf sides were probed. However, calculation of ETR is only applicable in the abaxial side which does not contain anthocyanins (Kytridis and Manetas, 2006). Anthocyanin presence in the palisade mesophyll introduces an uncertainty as to the actual PAR

reaching the probed chloroplasts, since anthocyanins also absorb in the blue band. The quantum yield of regulated non-photochemical energy loss, Φ_{NPQ}, was calculated as (F/F_M')–(F/F_M) and the quantum yield of non-regulated energy loss, Φ_{NO}, as F/F_M according to Hendrickson *et al.* (2004). Apparently, the quantum yields of photochemichal energy conversion and combined energy losses would sum to unity, i.e. $\Phi_{PSII}+\Phi_{NPQ}+\Phi_{NO}=1$.

Statistics

When appropriate, Student's *t*-test was used to assess significance of differences in the measured parameters between green and red leaves at each sampling date (SPSS 15.0 statistical package). In the case of pigment measurements, Student's *t*-test was performed separately for the 'green' and the 'red' period in order to assess significance of differences between green and red leaves.

Results

Pigments

Leaves of the red phenotype started turning red at late December. Anthocyanins displayed a steep initial increase to half-saturated levels within 4 d, followed by a more gradual increase up to a plateau reached in mid-February, and kept at high levels up to leaf senescence in mid-April (Fig. 1A). New leaves burst in mid-April and were green in both phenotypes. Chlorophyll ($a + b$) levels in the green period were similar in the two phenotypes and displayed an equal drop synchronized with the first appearance of anthocyanins in the red phenotype (Fig. 1B). Thereafter, greens recovered to previous levels, yet the reds remained at ~20–25% lower levels compared with the pre-reddening period. The chlorophyll *a*/*b* ratio was slightly higher in the green phenotype at almost all sampling dates, yet a lowering trend was evident in the reds during their 'red' period, resulting in a gradual increase in the percentage difference of greens over reds, as shown in Fig. 1C. Total carotenoids and the pools of xanthophyll cycle components (violaxanthin+antheraxanthin+zeaxanthin, VAZ) were consistently higher in the green phenotype during most of the sampling period, if expressed on a leaf area basis (D and E, respectively, in Fig. 1). The differences were more pronounced during the middle of the 'red' period. This was due to a stronger trend in the green phenotype to increase the photoprotective carotenoids during winter (Fig. 1E). When total carotenoids were expressed on a chlorophyll (Chl) basis no differences were observed between the two phenotypes (data not shown). When the VAZ/Chl and VAZ/total carotenoids ratios were computed (F and G, respectively, in Fig. 1), there was a slight, yet statistically significant, difference between the two phenotypes, with red leaves displaying lower ratios in the 'red' period. Finally, although the xanthophyll cycle pool size in the red leaves was lower, a trend for a lower mid-day epoxidation state was observed during the first half of the sampling period (Fig. 1H), i.e. the cycle seems to be more actively engaged at midday on clear days in the reds.

In vivo *fast transients of chlorophyll fluorescence in pre-darkened leaves*

The maximum (pre-dawn) efficiency of PSII photochemistry (φ_{Po} or F_V/F_M) of the green phenotype was high and constant at ~0.8 during the whole sampling period. In the red phenotype, a slight, yet significant trend for lower F_V/F_M values was observed ~2–3 weeks after the onset of reddening and kept up to the end of the red period in mid-spring (Fig. 2A). Much more pronounced differences between the two phenotypes were displayed in the parameters derived after further analysis of the fluorescence rise curves according to the JIP-test. Plotted on a logarithmic time scale, fluorescence rise curves were similar in the two phenotypes during the green and early red period (Fig. 3A), but quite different in the middle of the red period (Fig. 3B). Concomitantly, the derived parameters of photosystem structure and function were similar for the two leaf kinds during the green period and up to 2 weeks after the first signs of reddening (Figs 2, 3). After that date, parameters related to quantum yields or flux ratios (φ_{Eo}, φ_{Ro}, ψ_{Eo}, and δ_{Ro}; see Materials and methods for definitions) were considerably reduced in the red phenotype (Fig. 2). Concerning those parameters related to specific energy fluxes per active (Q_A-reducing) PSII reaction centre, these were either reduced (i.e. absorption, ABS/RC; trapped, TR/RC; electron transport, ET_0/RC) or remained constant (dissipation, DI_0/RC) in the green phenotype (Fig. 4). However, in the red phenotype, the parameters either increased (ABS/RC, TR/RC, DI_0/RC) or decreased to a lesser extent (ET_0/RC) during the red period. In Fig. 5, the relative amplitude of the I–P phase is given after normalization of the curves at the I-step. This amplitude gives a relative measure of the pool size of the final electron acceptors on the reducing side of PSI (Jiang *et al.*, 2008; Tsimilli-Michael and Strasser, 2008). As shown, the pool size is similar in both phenotypes during the green period (Fig. 5A), remains constant in the green phenotype during the red period but it declines considerably in the red phenotype after reddening (Fig. 5B). All differences in the chlorophyll fluorescence parameters were abolished after leaf re-greening at mid-spring. An additional measurement was performed in late winter to examine possible differences in chlorophyll fluorescence parameters obtained from the abaxial (shaded) leaf side. Results were qualitatively similar to those obtained from the adaxial (exposed) leaf side. Characteristic parameters are shown in Table 2.

Light dependence of PSII yield and development of the non-photochemical energy losses

Figure 6A indicates that light-acclimated PSII yield, Φ_{PSII}, obtained from the adaxial leaf side, is similar in the two leaf types, and the same is true for the light-dependent development of regulated, Φ_{NPQ}, and non-regulated, Φ_{NO},

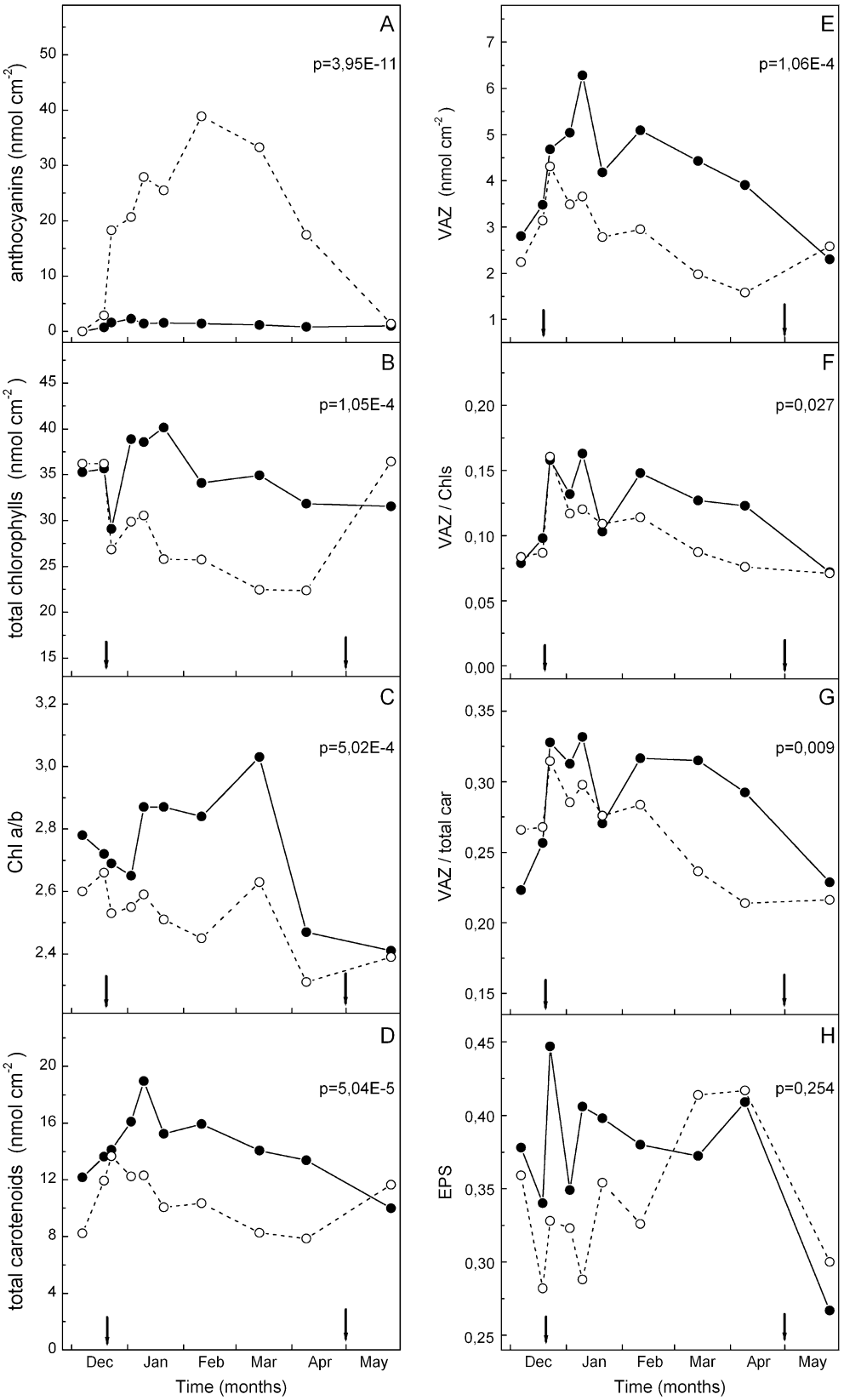

Fig. 1. Pigment levels and their ratios in green (closed circles) and red (open circles) phenotypes of *C. creticus* sampled on the dates indicated. The arrows denote the start and the end of the 'red' period. Leaves senesce and fall from mid-April to mid-May in parallel with new leaf emergence. During April, when old and new leaves co-occur, only old leaves (green and red, respectively) were sampled. The May sampling concerns new green leaves for both phenotypes. Values are means from two independent extractions per sampling date. Differences in each parameter between the two phenotypes are not significant during the 'green' period, but they are during the 'red' period, with the exception of the epoxidation state (EPS). *P*-values for the red period are inserted. VAZ=violaxanthin+antheraxanthin+zeaxanthin; EPS=(*V*+0.5*A*)/VAZ.

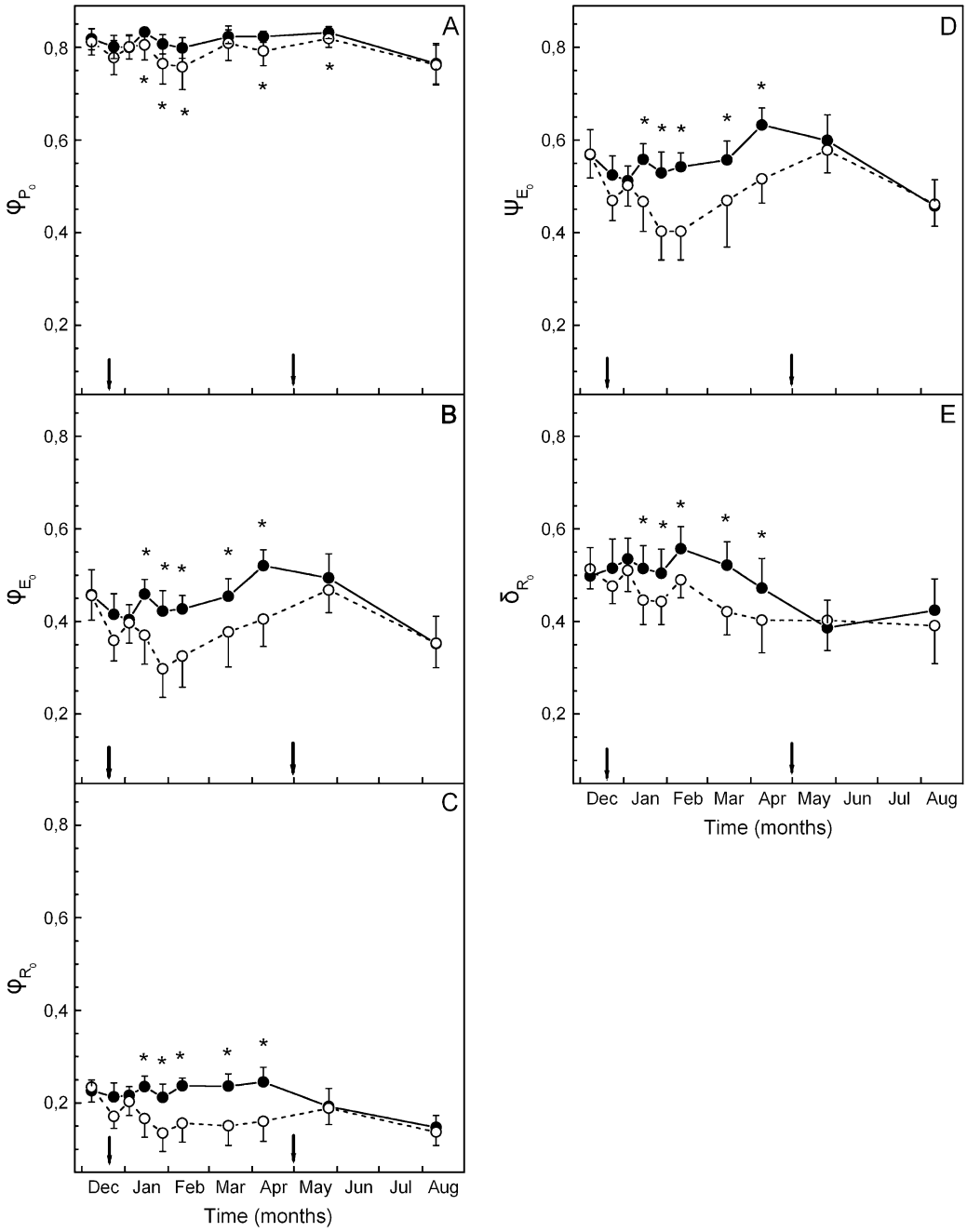

Fig. 2. Quantum yields of energy capture and electron flow as well as probabilities for trapped excitation energy to move electrons along the linear electron transport in green (closed circles) and red (open circles) phenotypes of *C. creticus* sampled on the dates indicated; φ_{P0} (equivalent to F_V/F_M), maximum quantum yield of primary photochemistry; φ_{E0}, quantum yield of electron transfer to intermediate carriers; φ_{R0}, quantum yield of reduction of electron acceptors of PSI; ψ_{E0}, efficiency to conserve trapped excitation energy to electron transfer; δ_{R0}, efficiency of electron transfer between reduced intermediate carriers to final electron acceptors of PSI. The arrows denote the start and the end of the 'red' period. Values are means ±standard deviation from five plants (six leaves per plant). The asterisks denote statistically significant (P <0.05) differences between the two phenotypes in the parameter indicated for each sampling date.

non-photochemical energy quenching (B and C, respectively, in Fig. 6). Corresponding measurements obtained from the lower leaf side (which does not contain anthocyanins) indicate that Φ_{PSII} of red leaves is considerably lower at all PAR levels tested (Fig. 6D). However, abaxial Φ_{NPQ} was higher in the red leaves at high PAR, while Φ_{NO} was higher at all PAR levels tested (E and F, respectively, in Fig. 6). In the case of the abaxial side which is devoid of anthocyanins, the accurate measurement of absorbed PAR (see Material and methods) permits the calculation of linear ETRs along PSII. As shown in Fig. 7, the values of ETR in red leaves at high PAR are lower.

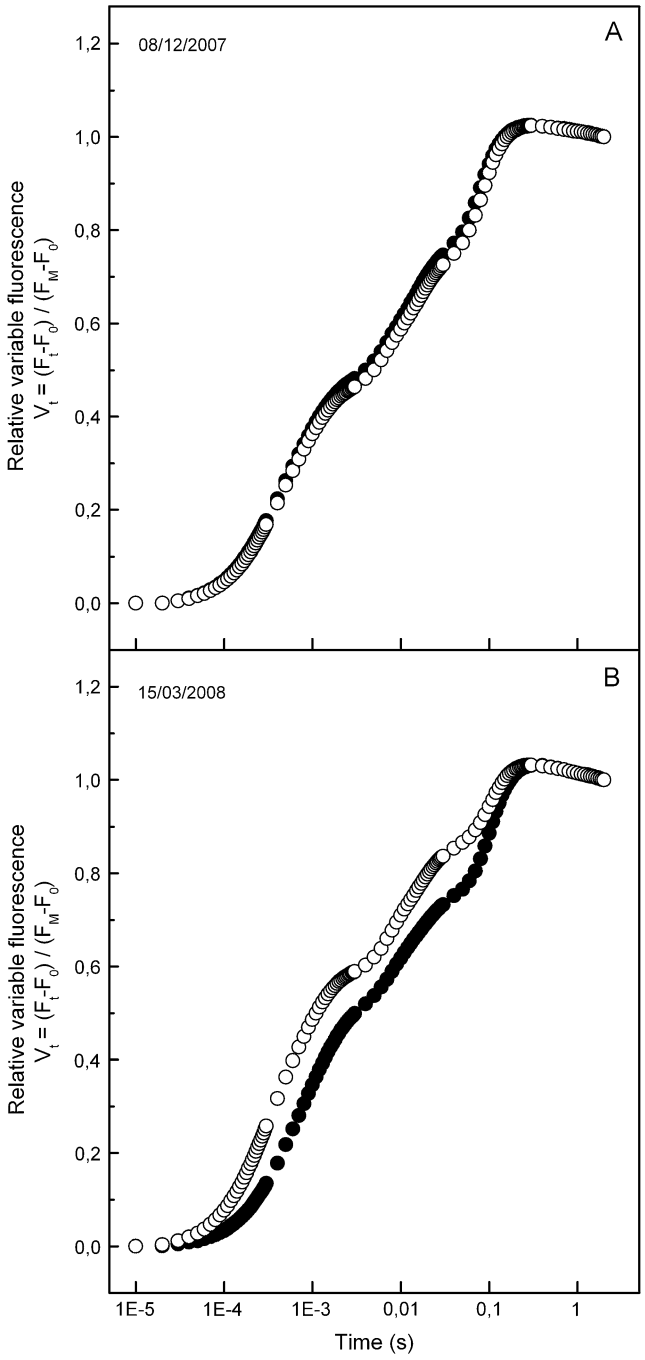

Fig. 3. Fast chlorophyll fluorescence transients of green (closed circles) and red (open circles) phenotypes sampled before (08/12/2007) and after (15/03/2008) leaf reddening of the red phenotype. Note the logarithmic time scale. On the vertical axis the relative variable fluorescence is given as $V_t=(F_t-F_0)/(F_M-F_0)$, i.e. after double normalization at F_0 and F_M. F_0 is the fluorescence yield at 20 μs. Values are means from five plants (six leaves per plant).

Discussion

The photoprotective hypothesis for leaf anthocyanins entails a lower photoinhibitory risk in the red leaves during the stressful period of the year. Mediterranean plants (García-Plazaola *et al.*, 1999), including *C. creticus* (Karavatas and Manetas, 1999), may suffer from sustained photoinhibition under cold winter temperatures combined with high light. However, assessing the mean photosynthetic behaviour in a population may hinder identification of intra-species differences between strong and weak phenotypes. In this investigation, it was shown that the green phenotype of *C. creticus* is more tolerant of winter photoinhibition while the red phenotype is quite sensitive. Traditionally, sustained photoihibition is assessed through measurements of maximum quantum yield of PSII photochemistry in dark-acclimated leaves. It has been argued, however, that this parameter (usually given as F_V/F_M or φ_{Po}) is not a sensitive indication of stress vulnerability (Strasser *et al.*, 2004). A high efficiency of exciton trapping indicates that primary photochemistry is not limiting, yet limitations in further steps of the excitation energy processing and its transformation to redox energy and electron transport may be hidden behind a high φ_{Po}. In the case of *C. creticus*, the green phenotype maintained the yield-related parameters (i.e. φ_{Po}, φ_{Eo}, φ_{Ro}, ψ_{Eo}, δ_{Ro}) almost constant during the whole sampling period (Fig. 2). Unexpectedly though, the corresponding parameters in the red phenotype dropped to lower values during late winter and early spring, in spite of anthocyanin accumulation (Fig. 2). The decline in φ_{Po} was minor (~7% difference between green and red leaves at most), confirming that primary photochemistry was not, in fact, limiting in the red phenotype. Corresponding differences in the other parameters of quantum yields depended on sampling date and ranged between ~20% for efficiency of electron flow from Q_A^- to intersystem electron carriers (φ_{Eo}) and ~30% for the rest of partial quantum yields. Hence, it can be concluded that the red-leaf phenotype suffers from a loss of photosynthetic activity during winter. Since the green/red differences in partial quantum yields are increasing along the linear electron flow from PSII to PSI (Fig. 2), an enhanced transformation of active PSII centres to non-Q_A- and/or non-Q-reducing centres can be inferred for the red phenotype. In addition, PSI is also negatively affected, as judged by the considerable reduction in the efficiency of electron transfer from intermediate carriers to final acceptors of PSI and the decline in the pools of these final acceptors (Figs 2C, E, 5). It can also be noted that the loss of photosynthetic activity in red leaves does not recover even after the full anthocyanin complement is realized in February. We consider that the above results weaken the photoprotective hypothesis, unless it is assumed that the target for protection is not related to photosynthesis. Alternatively, some photoprotection could be assumed, yet not enough to fully compensate for the higher vulnerability of the red phenotype to winter stress.

The conclusion for a lower photosynthetic activity in the red leaf phenotype is further strengthened by measurements of light-acclimated PSII yields of the upper leaf surface at various incident light levels (Fig. 6A). Although values of PSII effective yield, Φ_{PSII}, are only slightly (and non-significantly) lower in the red leaves, it has to be noted that PAR levels actually penetrating to red leaf mesophyll are in fact lower compared with their green counterparts, due to anthocyanin absorption of the blue actinic light used in

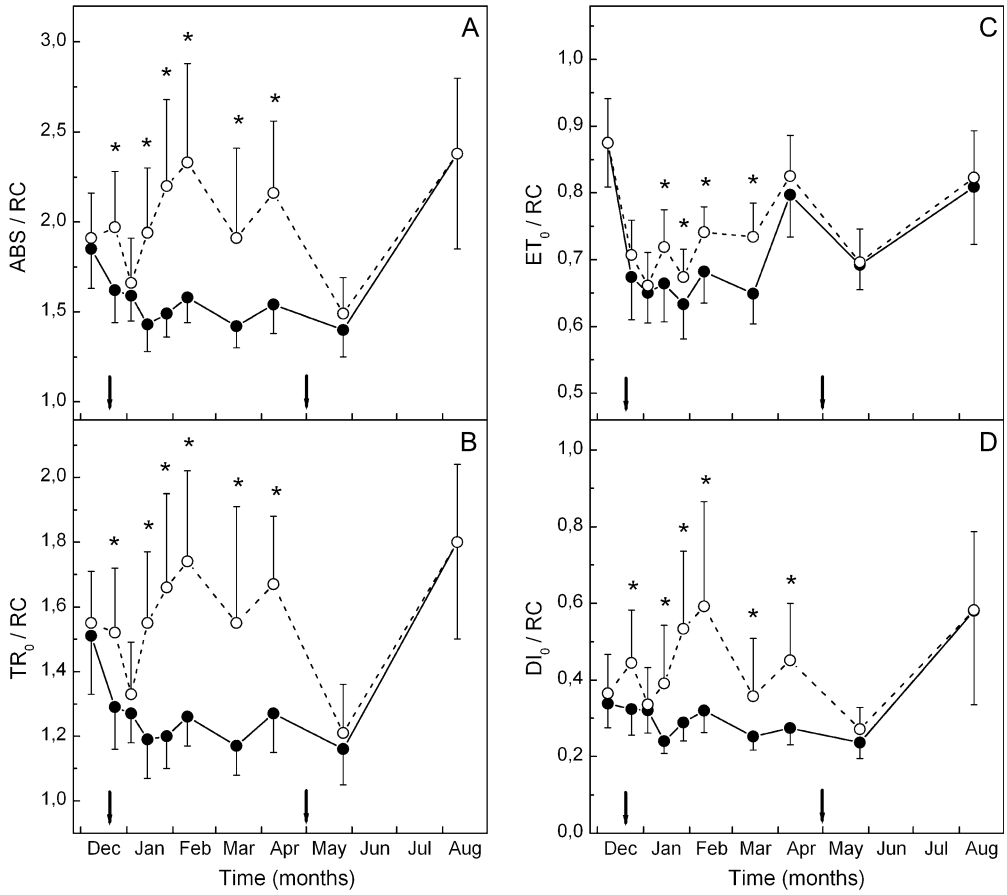

Fig. 4. Specific energy fluxes per active (i.e. Q_A-reducing) PSII reaction centre (RC) in green (closed circles) and red (open circles) phenotypes sampled on the dates indicated. The arrows denote the start and the end of the 'red' period. ABS, TR_0, ET_0, and DI_0 stand for absorbed energy, trapped energy, electron transport, and dissipated energy, respectively. Values are means ±standard deviation from five plants (six leaves per plant). The asterisks denote statistically significant (P <0.05) differences between the two phenotypes in the indicated parameter for each sampling date.

these measurements. Accordingly, for the same incident PAR, higher effective PSII yields would be expected in reds than greens. Instead of that, lower PSII yields were obtained. This is shown more clearly if the PSII effective yield and ETR are considered versus incident PAR obtained from the lower leaf surface when this surface is given actinic light (Figs 6D, 7). Under the conditions of this experiment, spongy mesophyll chloroplasts on both leaf types enjoy similar actual PAR (for a given incident PAR), since anthocyanins accumulate only in the palisade mesophyll (Kytridis and Manetas, 2006) and the abaxial leaf surface is always green. Figures 6D and 7 show that the lower leaf side of adaxially red leaves displays considerably lower Φ_{PSII} and ETR, especially at high PAR. Although lower effective PSII yield and ETR could be the result of a shade-acclimation syndrome of red leaves (see below), as would be expected for the lower leaf side due to the overlying anthocyanic screen, we point out that such an acclimation should not affect the maximum quantum yield of PSII photochemistry nor the quantum yields of partial electron flow reactions (see Table 2). These findings also reject the possibility that the alleged photoprotective function of leaf anthocyanins is targeted preferentially to the lower leaf surface.

Concomitant to the above may be the finding that the yield of regulated non-photochemical quenching, Φ_{NPQ}, of the adaxial surface is similar in the two leaf types, although one should expect a lower Φ_{NPQ} in red leaves due to the actually lower PAR reaching the palisade mesophyll (Fig. 6B). Corresponding values of Φ_{NPQ} obtained from the abaxial surface are significantly higher in red leaves at the higher PAR levels (Fig. 6E). This may be consistent with the lower midday epoxidation state of the xanthophyll cycle components in the red leaves during early winter (Fig. 1H), indicating a need for more active engagement of the cycle, in spite of the anthocyanic screen. Concerning the quantum yield of non-regulated energy loss, Φ_{NO}, this was significantly higher in the red leaves at all PAR levels (Fig. 6F). Since a high value of Φ_{NO} indicates vulnerability to photoinhibition (Hendrickson *et al.*, 2004), the assumption of an actual photoprotective function for leaf anthocyanins is further weakened.

Apart from the lower photosynthetic activity of red leaves suggested from the above results, a reduced photoprotective capacity is also evident if pigment levels and their changes are considered during the sampling period. Total carotenoids and the pool size of xanthophyll cycle

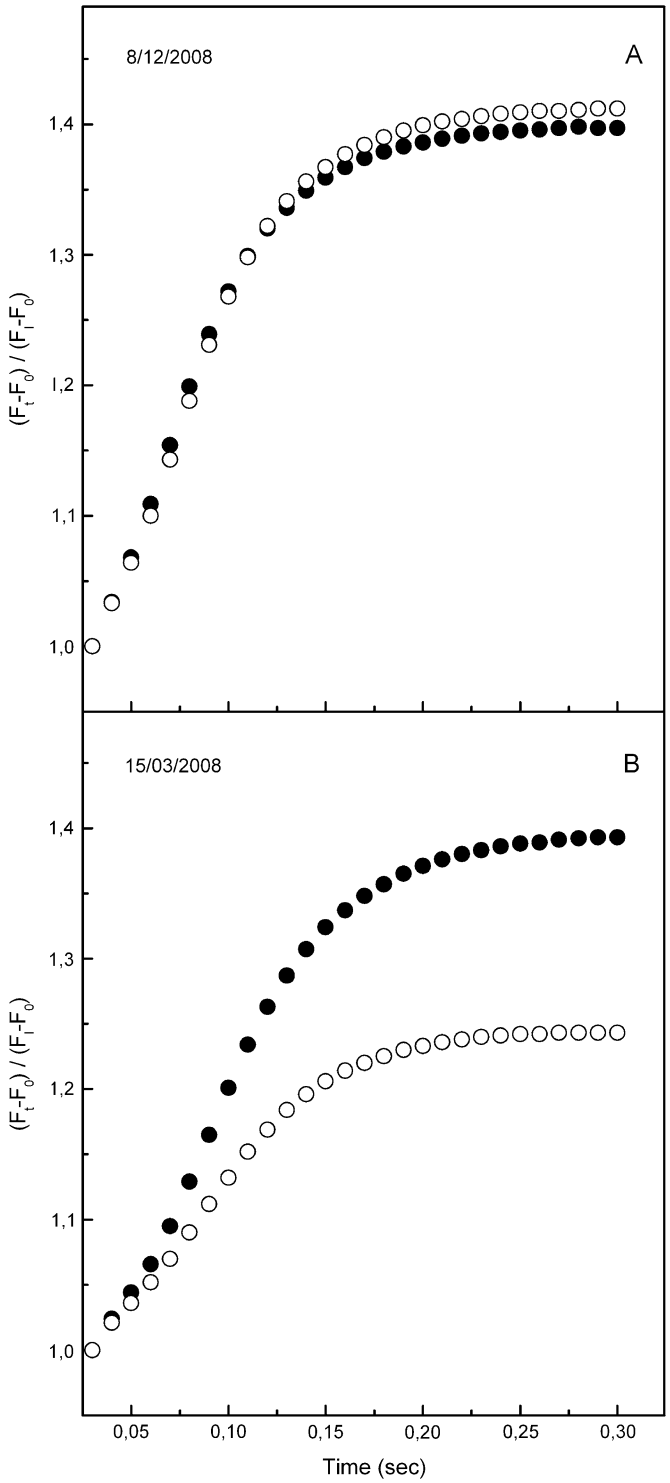

Fig. 5. Fluorescence rise kinetics of the I–P phase in green (closed circles) and red (open circles) phenotypes before (08/12/2007) and after (15/03/2008) leaf reddening of the red phenotype. On the vertical axis fluorescence is given as $(F_t–F_0)/(F_I–F_0)$, after normalization at F_I. F_0 and F_I stand for fluorescence yield at 20 μs and at 30 ms, respectively. Values are means from five plants (six leaves per plant).

components, expressed on a leaf area basis, were considerably lower in the red leaf phenotype throughout the sampling period and the differences became more pronounced during the red period (Fig. 1D, E). This is due to the strong increasing trend in both parameters during winter in the green leaves, while the capacity for such an increase in the reds is less evident. One may argue that a better way of expressing photoprotective carotenoid levels would be on a chlorophyll basis. Indeed the total carotenoids/Chl ratio was similar in the two leaf types throughout the sampling period, while the VAZ/Chl ratio became marginally lower in red leaves only during winter (Fig. 1F). This is due to the considerable decline in chlorophyll levels of the red leaves (Fig. 1B). We argue, however, that the crucial parameter in photoprotection by carotenoids may not be the concentration of the target molecules (chlorophylls) but their absorptance. Leaf absorptance is a weak function of chlorophyll levels, especially when these levels are normal. Thus, a 50% decrease in Chl results in a ~10% decrease in leaf absorptance (Dima *et al.*, 2006) due to the sieve effect observed in heterogeneous, chlorophyll-containing tissues (Vogelmann, 1993). It can therefore be concluded that the photoprotective capacity of the red-leaf phenotype is smaller. This photoprotective inefficiency, together with the report that the nitrogen content in the red phenotype of *C. creticus* is also lower (Kytridis *et al.*, 2008) may underlie the observed decline of photosynthetic activity during winter. According to the above, we could suggest that Chl loss, combined with anthocyanin accumulation, may have the adaptive significance of reducing (albeit slightly) the excitation pressure in the chloroplasts of the red leaf phenotype. Nevertheless, their additive effect may not be enough to alleviate photosynthetic inactivation fully. Increases in xanthophyll cycle pool sizes and chlorophyll loss have been reported as part of an adaptive repertoire of Mediterranean plants during adverse environmental conditions (Kyparissis *et al.*, 1995, 2000). Red leaves of *C. creticus* display a capacity for Chl loss, but not for an increase in carotenoids. Thus, even if anthocyanins exert a photoprotective function, their effect is slight.

It has been repeatedly argued that an anthocyanic screen would lead to a shade acclimation of photosynthesis (Gould *et al.*, 2002; Manetas *et al.*, 2003; Hughes and Smith, 2007; Kyparissis *et al.*, 2007). Ample evidence for an apparent shade acclimation was also obtained in this investigation. Some of the evidence, however, could be partly linked to the higher sensitivity of the red phenotype to the

Table 2. Chlorophyll fluorescence parameters obtained from the abaxial (lower) leaf side of leaves of the green and red phenotype in late winter

Data are means ±standard deviation from 10 leaves (two leaves/shrub). Differences in each parameter between the two phenotypes are statistically significant (P <0.05), with the exception of φ_{Po}.

Fluorescence parameter	Green leaves	Red leaves
φ_{Po}	0.838±0.011	0.822±0.024
φ_{Eo}	0.507±0.044	0.392±0.063
φ_{Ro}	0.201±0.028	0.132±0.026
ψ_{Eo}	0.605±0.048	0.476±0.064
δ_{Ro}	0.396±0.049	0.337±0.035
ABS/RC	1.947±0.158	2.385±0.446

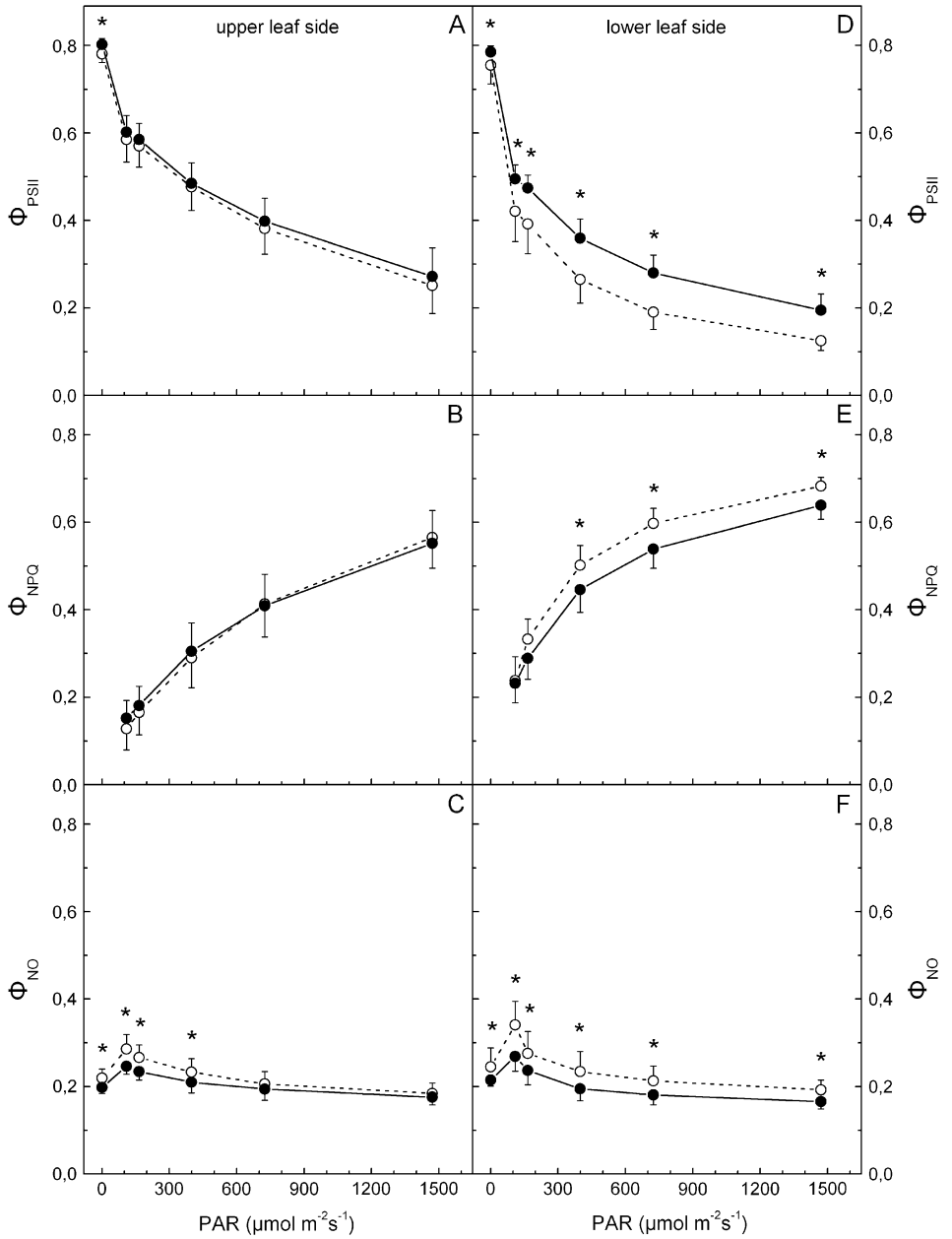

Fig. 6. Changes in light-acclimated PSII effective yield, Φ_{PSII}, and non-photochemical energy quenching (either regulated, Φ_{NPQ}, or non-regulated, Φ_{NO}), versus incident light level, in green (closed circles) or red (open circles) leaves. The experiment was performed during the 'red' period (5 March 2008) and the left and right panels refer to values obtained from the upper and lower leaf side, respectively. The leaves remained under the indicated PAR until stable values for each parameter were obtained. Values are means ±standard deviation from five plants (four leaves per plant). The asterisks denote statistically significant (P <0.05) differences between the two phenotypes in the parameter indicated for each PAR level.

superimposed winter stress. Hence, the lower ratios of VAZ/total carotenoids in the red leaves during winter could be interpreted either as part of the shade acclimation syndrome (Thayer and Björkman, 1990) or as an inherent inability of the red phenotype to up-regulate the xanthophyll pool size (Fig. 1E, G). Moreover, the enhanced mean antenna size (as judged by the specific flux of light absorption per reaction centre, ABS/RC) is an indication of shade acclimation (Anderson, 1986) and it was shown in this study to increase considerably after anthocyanin accumulation (Fig. 4A). Yet, according to the assumptions of the JIP-test (Strasser *et al.*, 2004), the antenna size is expressed per active (i.e. Q_A-reducing) PSII centre. Hence, the increase in this parameter could be the combined effect of an increase in the antenna size and a decrease in active PSII centres. However, the diminishing Chl *a*/*b* ratios (Fig. 1C) can be better accommodated within an assumed shade acclimation in red leaves, than interpreted on the basis of their higher winter stress sensitivity (Anderson, 1986).

In conclusion, this investigation demonstrated that the red leaf phenotype of the evergreen *C. creticus* is inherently more sensitive to winter stress, displaying a reduction in

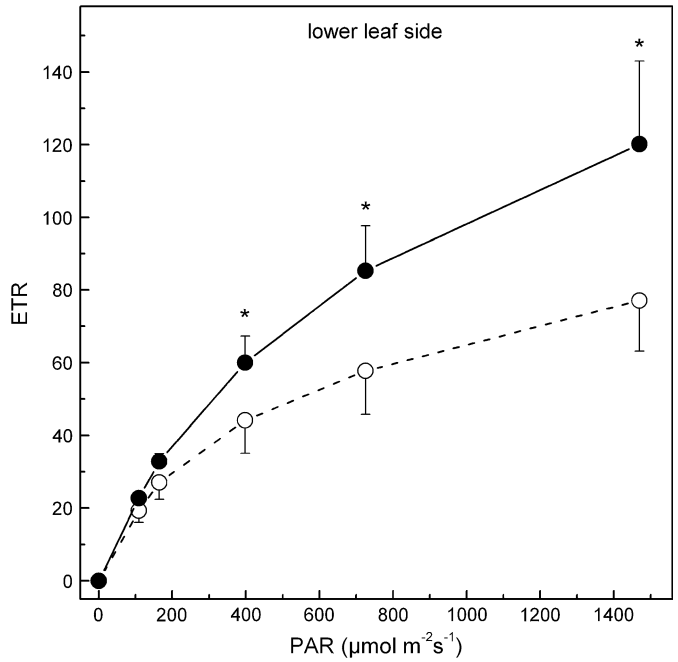

Fig. 7. Linear electron transport rates (ETR) along PSII in the lower leaf side of green (closed circles) and red (open circles) phenotypes. The experiment was performed during the 'red' period (5 March 2008). The leaves remained under the indicated PAR until stable values for each parameter were obtained. Values are means ±standard deviation from five plants (four leaves per plant). The asterisks denote statistically significant (P <0.05) differences between the two phenotypes in the parameter indicated for each PAR level.

electron flow in both photosystems and a difficulty in improving the photoprotective potential based on the xanthophyll cycle components, in spite of the higher need for non-photochemical quenching. Anthocyanin accumulation and the concomitant chlorophyll loss may afford some protection by reducing excitation pressure and increasing the anti-oxidative potential, yet not to the extent of a full photosynthetic competence with the green phenotype.

Appendix

Cardinal points in the kinetics of fast chlorophyll fluorescence rise and the formulae used for the calculation of biophysical parameters, according to the JIP-test.

F_0	$F_{20\mu s}$, fluorescence intensity at 20 μs, considered as the fluorescence intensity when all reaction centres (RC) are open
F_M	Maximal fluorescence intensity, considered as the fluorescence intensity when all RCs are closed
F_V	Variable fluorescence, F_M–F_0
F_J or F_I	Fluorescence intensity at 2 ms or 30 ms, respectively
M_0 or $(dV/dt)_0$	$4(F_{300\mu s}–F_0)/(F_M–F_0)$, initial slope of the fluorescence transient
V_J	$(F_{2ms}–F_0)/(F_M–F_0)$, relative variable fluorescence at 2 ms
V_I	$(F_{30ms}–F_0)/(F_M–F_0)$, relative variable fluorescence at 30 ms
Quantum yields or flux ratios	
φ_{Po} or TR_0/ABS	$F_V/F_M=1–F_0/F_M$
φ_{Eo} or ET_0/ABS	$\varphi_{Po}\cdot\psi_{Eo}=1–F_J/F_M$
φ_{Ro}	$\varphi_{Po}\cdot\psi_E\cdot\delta_{Ro}=1–F_I/F_M$
ψ_{Eo} or ET_0/TR_0	$1–V_J=(F_M–F_J)/(F_M–F_0)$
δ_{Ro}	$(1–V_I)/(1–V_J) = (F_M–F_I)/(F_M–F_J)$
Specific energy fluxes per RC	
ABS/RC	$(M_0/V_J)\cdot F_M/(F_M–F_0)$
TR_0/RC	M_0/V_J
ET_0/RC	$(M_0/V_J)\cdot(1–V_J)$
DI_0/RC	$(M_0/V_J)\cdot(F_0/F_V)$

Acknowledgements

We thank the Research Committee of the University of Patras (project K Karatheodori) for funding this work.

References

Anderson JM. 1986. Photoregulation of the composition, function, and structure of thylakoid membranes. *Annual Review of Plant Physiology and Plant Molecular Biology* **37,** 93–136.

Archetti M. 2000. The origin of autumn colours. *Journal of Theoretical Biology* **205,** 625–630.

Archetti M, Leather SR. 2005. A test of the coevolution theory of autumn colours: colour preference of *Rhopalosiphum padi* on *Prunus padus*. *Oikos* **110,** 339–343.

Burger J, Edwards GE. 1996. Photosynthetic efficiency, and photodamage by UV and visible radiation, in red versus green leaf in *Coleus varieties*. *Plant and Cell Physiology* **37,** 395–399.

Esteban R, Fernández-Marín B, Becerril JM, García-Plazaola JI. 2008. Photoprotective implications of leaf variegation in *E. dens-canis* L. and *P. officinalis* L. *Journal of Plant Physiology* **165,** 1255–1263.

Dima E, Manetas Y, Psaras GK. 2006. Chlorophyll distribution pattern in inner stem tissues: evidence from epifluorescence microscopy and reflectance measurements in 20 woody species. *Trees* **20,** 515–521.

Feild TS, Lee DW, Holbrook M. 2001. Why leaves turn red in autumn: the role of anthocyanins in senescing leaves of red-osier dogwood. *Plant Physiology* **127,** 566–574.

García-Plazaola JI, Artetxe U, Dunabeitia MK, Becceril JM. 1999. Role of photoprotective systems of holm-oak (*Quercus ilex*) in the adaptation to winter conditions. *Journal of Plant Physiology* **155,** 625–630.

Genty B, Briantais J-M, Baker NR. 1989. The relationship between quantum yield of photosynthetic electron transport rate and quenching of chlorophyll fluorescence. *Biochimica et Biophysica Acta* **990,** 87–92.

Gould KS, Vogelmann TC, Han T, Clearwater MJ. 2002. Profiles of photosynthesis within red and green leaves of *Quintinia serrata* A. Cunn. *Physiologia Plantarum* **116,** 127–133.

Hamilton WD, Brown SP. 2001. Autumn tree colours as a handicap signal. *Proceedings of the Royal Society of London B: Biological Sciences* **268,** 1489–1493.

Hendrickson L, Furbank RT, Chow WS. 2004. A simple alternative approach to assessing the fate of absorbed light energy using chlorophyll fluorescence. *Photosynthesis Research* **82,** 73–81.

Hughes NM, Neufeld HS, Burkey KO. 2005. Functional role of anthocyanins in high-light winter leaves of the evergreen herb *Galax urceolata*. *New Phytologist* **168,** 575–587.

Hughes NM, Smith WK. 2007. Attenuation of incident light in *Galax urceolata* (Diapensiaceae): concerted influence of adaxial and abaxial anthocyanic layers on photoprotection. *American Journal of Botany* **94,** 784–790.

Jiang HX, Chen LS, Zheng JG, Han S, Tang N, Smith BR. 2008. Aluminum-induced effects on Photosystem II photochemistry in *Citrus* leaves assessed by the chlorophyll *a* fluorescence transient. *Tree Physiology* **28,** 1863–1871.

Karageorgou P, Manetas Y. 2006. The importance of being red when young: anthocyanins and the protection of young leaves of *Quercus coccifera* from insect herbivory and excess light. *Tree Physiology* **26,** 613–621.

Karavatas S, Manetas Y. 1999. Seasonal patterns of photosystem 2 photochemical efficiency in evergreen sclerophylls and drought semi-deciduous shrubs under Mediterranean field conditions. *Photosynthetica* **36,** 41–49.

Krol M, Gray GR, Hurry VM, Oquist G, Malker L, Huner NPA. 1995. Low-temperature stress and photoperiod affect an increased tolerance to phoinhibition in *Pinus banksiana* seedlings. *Canadian Journal of Botany* **73,** 1119–1127.

Kyparissis A, Drilias P, Manetas Y. 2000. Seasonal fluctuations in photoprotective (xanthophyll cycle) and photoselective (chlorophylls) capacity in eight Mediterranean plant species belonging to two different growth forms. *Australian Journal of Plant Physiology* **27,** 265–272.

Kyparissis A, Grammatikopoulos G, Manetas Y. 2007. Leaf morphological and physiological adjustments to the spectrally selective shade imposed by anthocyanins in *Prunus cerasifera*. *Tree Physiology* **27,** 849–857.

Kyparissis A, Petropoulou Y, Manetas Y. 1995. Summer survival of leaves in a soft-leaved shrub (*Phlomis fruticosa* L., Labiatae) under Mediterranean field conditions: avoidance of photoinhibitory damage through decreased chlorophyll contents. *Journal of Experimental Botany* **46,** 1825–1831.

Kytridis V-P, Karageorgou P, Levizou E, Manetas Y. 2008. Intraspecies variation in transient accumulation of leaf anthocyanins in *Cistus creticus* during winter: evidence that anthocyanins may compensate for an inherent photosynthetic and photoprotective inferiority of the red-leaf phenotype. *Journal of Plant Physiology* **165,** 952–959.

Kytridis V-P, Manetas Y. 2006. Mesophyll versus epidermal anthocyanins as potential *in vivo* antioxidants: evidence linking the putative antioxidant role to the proximity of oxy-radical source. *Journal of Experimental Botany* **57,** 2203–2210.

Lee DW, Gould KS. 2002. Anthocyanins in leaves and other vegetative organs: an introduction. *Advances in Botanical Research* **37,** 1–16.

Lee DW, O'Keefe J, Holbrook NM, Feild TS. 2003. Pigment dynamics and autumn leaf senescence in a New England deciduous forest, eastern USA. *Ecological Research* **18,** 677–694.

Liakopoulos G, Nikolopoulos D, Klouvatou A, Vekkos K-A, Manetas Y, Karabourniotis G. 2006. The photoprotective role of epidermal anthocyanins and surface pubescence in young leaves of grapevine (*Vitis vinifera*). *Annals of Botany* **98,** 257–265.

Licthenthaler HK, Wellburn AR. 1983. Determinations of total carotenoids and chlorophylls *a* and *b* of leaf extracts in different solvents. *Biochemical Society Transactions* **11,** 591–592.

Lindoo SJ, Caldwell MM. 1978. Ultraviolet-B radiation-induced inhibition of leaf expansion and promotion of anthocyanin production – lack of involvement of low irradiance phytochrome system. *Plant Physiology* **61,** 278–282.

Manetas Y. 2006. Why some leaves are anthocyanic and why most anthocyanic leaves are red? *Flora* **201,** 163–177.

Manetas Y, Drinia A, Petropoulou Y. 2002. High contents of anthocyanins in young leaves are correlated with low pools of xanthophyll cycle components and low risk of photoinhibition. *Photosynthetica* **40,** 349–354.

Manetas Y, Petropoulou Y, Psaras GK, Drinia A. 2003. Exposed red (anthocyanic) leaves of *Quercus coccifera* display shade characteristics. *Functional Plant Biology* **30,** 265–270.

Ougham HJ, Morris P, Thomas H. 2005. The colors of autumn leaves as symptoms of cellular recycling and defenses against environmental stresses. *Current Topics in Developmental Biology* **66,** 135–160.

Ougham HJ, Thomas H, Archetti M. 2008. The adaptive value of leaf colour: origin and evolution of autumn colours. *New Phytologist* **179,** 9–13.

Papageorgiou GC, Tsimilli-Michael M, Stamatakis K. 2007. The fast and slow kinetics of chlorophyll *a* fluorescence induction in plants, algae and cyanobacteria: a viewpoint. *Photosynthesis Research* **94,** 275–290.

Pietrini F, Iannelli MA, Massacci A. 2002. Anthocyanin accumulation in the illuminated surface of maize leaves enhances protection from photo-inhibitory risks at low temperature, without further limitation to photosynthesis. *Plant, Cell & Environment* **25,** 1251–1259.

Steyn WJ, Wand SJE, Holcroft DM, Jacobs G. 2002. Anthocyanins in vegetative tissues: a proposed unified function in photoprotection. *New Phytologist* **155,** 349–361.

Strasser RJ, Srivastava A, Govindjee. 1995. Polyphasic chlorophyll *a* fluorescence transient in plants and cyanobacteria. *Photochemistry and Photobiology* **61,** 32–42.

Strasser RJ, Tsimilli-Michael M, Srivastava A. 2004. Analysis of the chlorophyll *a* fluorescence transient. In: Papageorgiou GC, Govindjee, eds. *Chlorophyll fluorescence: a signature of photosynthesis*. Advances in photosynthesis and respiration series, Vol. 19. Rotterdam: Kluwer, 321–362.

Thayer SS, Björkman O. 1990. Leaf xanthophyll content and composition in sun and shade determined by HPLC. *Photosynthesis Research* **23,** 331–343.

Tsimilli-Michael M, Strasser RJ. 2008. *In vivo* assessment of plants' vitality: applications in detecting and evaluating the impact of mycorrhization on host plants. In: Varma A, ed. *Mycorrhiza: state of the art, genetics and molecular biology, eco-function, biotechnology, eco-physiology, structure and systematics*, 3rd edn. Berlin: Springer, 679–703.

Vogelmann TC. 1993. Plant tissue optics. *Annual Review of Plant Physiology and Plant Molecular Biology* **44,** 231–251.

Yordanov I, Goltsev V, Stefanov D, Chernev P, Zaharieva I, Kirova M, Gecheva V, Strasser RJ. 2008. Preservation of photosynthetic electron transport from senescence-induced inactivation in primary leaves after decapitation and defoliation of bean plants. *Journal of Plant Physiology* **165,** 1954–1963.